



Decolorization of methyl green and bromocresol purple in mono and binary systems by photochemical processes: direct UV photolysis, Acetone/UV and H₂O₂/UV. A comparative study

I. Bousnoubra^a, K. Djebbar^{a,*}, A. Abdessemed^{a,b}, T. Sehili^a

^aLaboratory Science and Technology Environment, Faculty of Sciences, Department of Chemistry, University of Constantine, Constantine, Algeria, emails: ibtissembousnoubra@gmail.com (I. Bousnoubra), kedjebbar@yahoo.fr (K. Djebbar), ala.abdessemed@gmail.com (A. Abdessemed), tsehili@yahoo.fr (T. Sehili)

^bBiotechnology Research Centre, BPE 73, Ali Mendjeli, Nouvelle Ville, 25000 Constantine, Algeria

Received 6 October 2015; Accepted 27 March 2016

ABSTRACT

The aim of this study is to test the ability of photochemical processes (photolysis, Acetone/UV and H₂O₂/UV at 254 nm) to eliminate the Methyl Green (MG, cationic structure) and Bromocresol Purple (BCP, anionic structure) in aqueous solution in mono and binary systems. The obtained results show that the rate of decolorization by UV photolysis at 254 nm in single system is weak for BCP (25%) and acceptable for MG (66%). In dark conditions, preliminary experiments show no decolorization of the two dyes in the presence of acetone and in the presence of H₂O₂ for BCP. However, classical oxidation has been observed for MG in H₂O₂ for concentrations superior to 5×10^{-4} M. In the presence of light, a real improvement in the decolorization rate of both dyes is obtained using H₂O₂/UV (acting via ·OH issued from photolysis of H₂O₂ at 254 nm) and Acetone/UV (acting via energy transfer from the sensitizer which is Acetone to the dye). In the mixture systems, the Acetone/UV process is more effective than direct UV photolysis and H₂O₂/UV. In the three photochemical processes used, each dye decreases the removal efficiency of the other. The dyes removal kinetics follows the pseudo-first-order model in Acetone/UV and H₂O₂/UV systems for both dyes in single and binary systems.

Keywords: Degradation; MG; BCP; Irradiation; Acetone; H₂O₂

1. Introduction

The considerable release of dyes from textile industries, tanneries, printing activities, etc is a major problem of pollution because they can destroy aquatic life (fauna and flora) and may cause a real threat to human health as most of these substrates are toxic and carcinogenic [1–3]. Their decontamination is carried out

via chemical techniques which have already been developed in the past: biological methods [4,5], ion exchange [6,7], adsorption on various supports such as: clay, activated carbon, and semi conductors [8–12]. Unfortunately, these techniques are inefficient since they may be prejudicial to environment. The processes, like adsorption and ion exchange two common methods used in the treatment of wastewater, are not effective because they result in solid waste due to the transfer of the pollution from one phase to another.

*Corresponding author.

In addition, it is important to mention that solid waste may become the pollutant itself. Thus, expensive post treatments are required like: incineration and land filling. Furthermore, we observe also a resistance to biodegradation for dyes having complicated structure which are characterized by the presence of many aromatic cycles [13]. It can be stated that such treatment can lead to an incomplete degradation as several dyes are resistant to microbial attack, stable to light and temperature. However, some processes like the enzymatic systems which are available, are able to degrade harmful products such as pesticides, chlorinated phenols, polycyclic aromatic hydrocarbons, and dyes [14]. Other degradation processes like chemicals methods are very expensive as they require high dosage and may generate large amount of sledges [15].

In these later decades, photochemical systems, mainly, the advanced oxidation processes (AOPs), are innovative and alternative techniques for wastewater treatment. This effectiveness is related to the production of highly reactive species: the radicals $\cdot\text{OH}$. They may react rapidly with a high rate constant (10^7 – $10^{10} \text{ M}^{-1}\text{s}^{-1}$) and non selectively with a broad range of organic pollutants [16]. Thus, a process of oxidation takes place until the final stage of mineralization which is characterized by the production of CO_2 and H_2O_2 . AOPs include several processes in homogeneous medium: $\text{Fe}^{2+}/\text{H}_2\text{O}_2$, $\text{Fe}^{3+}/\text{H}_2\text{O}_2$, $\text{Fe}^{2+}/\text{H}_2\text{O}_2/\text{UV}$, $\text{H}_2\text{O}_2/\text{UV}$, $\text{Fe}^{3+}/\text{H}_2\text{O}_2/\text{UV}$... and in heterogeneous medium: UV/Semi-conductors [17–24].

In this study, we present results obtained from the use of photochemical systems (direct UV photolysis, acetone/UV and $\text{H}_2\text{O}_2/\text{UV}$) in the decolorization process of two dyes (Methyl Green and Bromocresol Purple) used in mono and binary systems in aqueous homogeneous phase. The UV–vis spectral changes of MG and BCP taken separately will be examined. In addition, the influence of some parameters, like dyes, H_2O_2 and Acetone concentrations, will be investigated in both cases.

In addition, it is interesting to make a comparison of the obtained results with other related studies. To the best of our knowledge, the information on topic related to the decolorization of dye mixtures using photosensitivity and other processes in homogeneous phase is limited. Hence, this investigation may represent an important part of this work.

2. Experimental

2.1. Materials

Methyl Green and Bromocresol Purple are purchased from Fluka chemical company and used

without further purification. The hydrogen peroxide (33% Fluka), Sodium persulfate ($\text{Na}_2\text{S}_2\text{O}_8$, Prolabo), and Acetone ($\text{C}_3\text{H}_6\text{O}$ $d = 0.79$, Labosi) solutions are prepared with ultra pure water from a Milli pure water (Milli-Q purification unit). The structure of our both substrates is represented in Fig. 1. We notice that initial concentration is 25 ppm for both dyes and the natural pH is equal to 5.8 for MG and 4.5 for BCP.

2.2. Photoreactor and source light

Different aqueous solutions are irradiated at 254 nm in cylindrical reactor in quartz (100 cm of length and 2 cm in diameter), located on one of the principal axis of the assembly, and equipped with three symmetrical external low-pressure mercury lamps (germicide lamp, Philips TUV 15 W) emitting mainly at 254 nm. The reactor is surrounded symmetrically by these lamps. The temperature of the reactor is maintained between 18 and 20°C by the use of an air flow provided by a ventilator. The entire system is placed in a cylindrical enclosure [25].

2.3. Analysis method

The UV–vis spectra of both dyes are recorded from 200 to 800 nm using a spectrophotometer “Unicam Helios α ” with a cell made in quartz and having a path length of 1 cm. The residual concentrations of both substrates at different irradiation times are obtained at $\lambda_{\text{max}} = 632 \text{ nm}$ for MG and at $\lambda_{\text{max}} = 432 \text{ nm}$ for BCP, from their calibration curve. In the mixture, determination of the concentration is carried out according to the following relation [26]:

$$C_1 = \frac{(\varepsilon_2^2 A^2 - \varepsilon_2^1 A^1)}{(\varepsilon_1^1 \varepsilon_2^2 - \varepsilon_2^1 \varepsilon_1^2)} \times 1 \quad (1)$$

$$C_2 = \frac{(\varepsilon_1^1 A^2 - \varepsilon_1^2 A^1)}{(\varepsilon_1^1 \varepsilon_2^2 - \varepsilon_2^1 \varepsilon_1^2)} \times 1 \quad (2)$$

with C_1 : Concentration of the dye (1); C_2 : Concentration of the dye (2); A^1 : Absorbance measured at the wavelength of the absorption maximum of the dye (1); A^2 : Absorbance measured at the wavelength of the absorption maximum of the dye (2); ε_1^1 : specific extinction coefficient of the dye (1) at its absorption maximum; ε_2^1 : specific extinction coefficient of the dye (1) at the absorption maximum of dye (2); ε_2^2 : specific extinction coefficient of the dye (2) at its absorption maximum; ε_1^2 : specific extinction coefficient of the dye (2) at

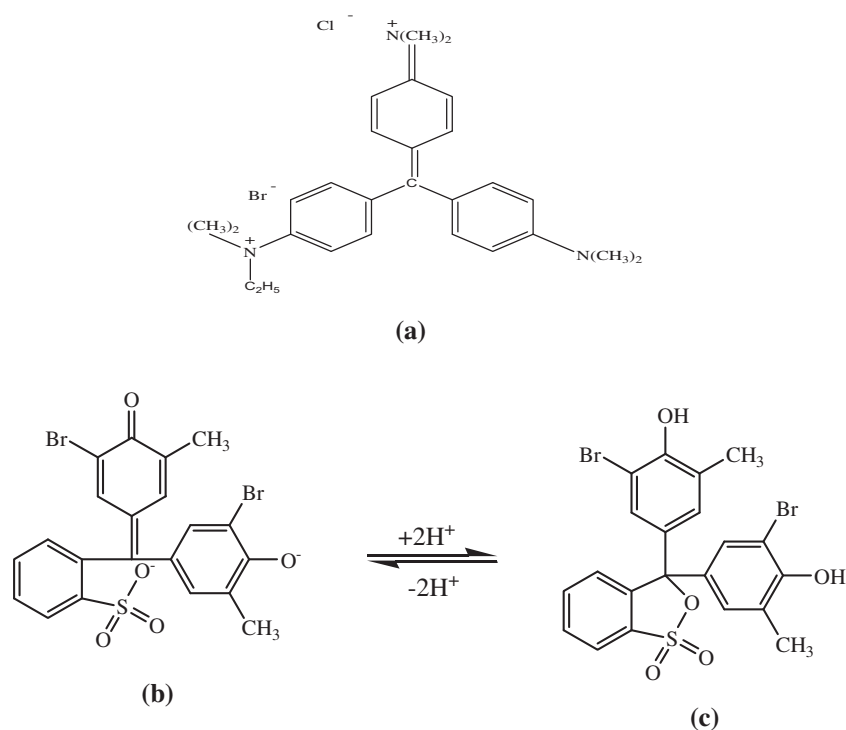


Fig. 1. (a) Molecule structure of Methyl Green (MG), (b) Molecule structure of Bromocresol Purple (BCP) The BCP exists under equilibrium state between two forms: (b) and (c). In our experimental conditions (pH 4.5), the dominant form is the species “c”.

the absorption maximum of dye (1); l : thickness of the cell (1 cm).

3. Results and discussion

3.1. Case of single dye

3.1.1. UV-vis spectrum of MG and BCP

The UV-vis spectra of MG and BCP are presented in Fig. 2(a) and (b). It is clear that MG (pH 5.8) absorbs light in the range of wavelength: 200–700 nm and shows an intense band located around 632 nm ($\epsilon = 16,250 \text{ L mol}^{-1} \text{ cm}^{-1}$) with three other bands less intense located, respectively, around 254 nm ($\epsilon = 2,470 \text{ L mol}^{-1} \text{ cm}^{-1}$), 312 nm ($\epsilon = 4,690 \text{ L mol}^{-1} \text{ cm}^{-1}$), and 420 nm ($\epsilon = 2,780 \text{ L mol}^{-1} \text{ cm}^{-1}$). Similar evolution is observed with BCP (pH 4.5) which exhibits also an intense peak situated around 276 nm ($\epsilon = 15,930 \text{ L mol}^{-1} \text{ cm}^{-1}$) and a less intense one at 432 nm ($\epsilon = 28,246 \text{ L mol}^{-1} \text{ cm}^{-1}$). It can be seen that pH affects spectrum of each dye. Thus, in basic solution (pH 10.00), a complete decolorization of MG is obtained and can be attributed to classical oxidation whereas for BCP, a shift to a higher wavelength occurs for the band positioned at 432 nm. This shift is equal to 588 nm and

involves a bathochromic effect, with a color change (turning into violet). In acidic solution (pH 2.00), the most intense band increases in the case of PCB and decreases slightly in the case of MG. Additionally, no shift and no color change are observed for both substrates. According to these conditions, we may determine the pK_a of acid/Base couple of this dye where its magnitude of order is about 6.1 (insert in Fig. 2(b)).

3.1.2. Direct photolysis of MG and BCP

Fig. 3(a) and (b) present typical data obtained from the photolysis of MG ($[MG]_0 = 25 \text{ mg/L}$) and BCP ($[BCP]_0 = 25 \text{ mg/L}$) in aerated medium, in a tubular reactor, and under UV irradiation at 254 nm. The experimental results show that the MG removal reaches 66% after a long reaction time: 240 min whereas only 25% of PCB is removed in the same time. For MG, the photoproducts are formed, mainly, in the beginning of the photolytic process, for a time ranging from 0 to 25 min (no attempt is performed to identify them). Thus, these results show that the elimination of MG is superior to that of BCP and indicate that MG absorbs light better than BCP. Consequently,

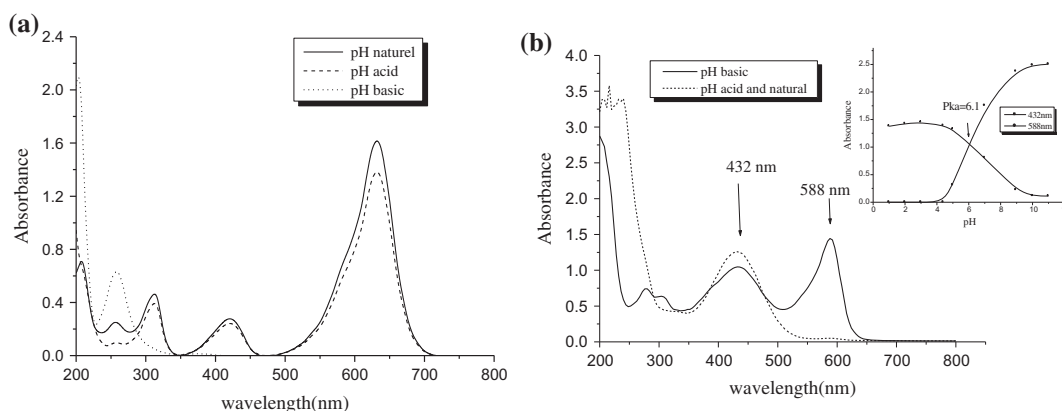


Fig. 2. UV-vis spectra of dyes at different pH ($[dye]_0 = 25$ ppm): (a) MG and (b) BCP (In inset: evolution of absorbance vs. pH: determination of the pK_a for PCB).

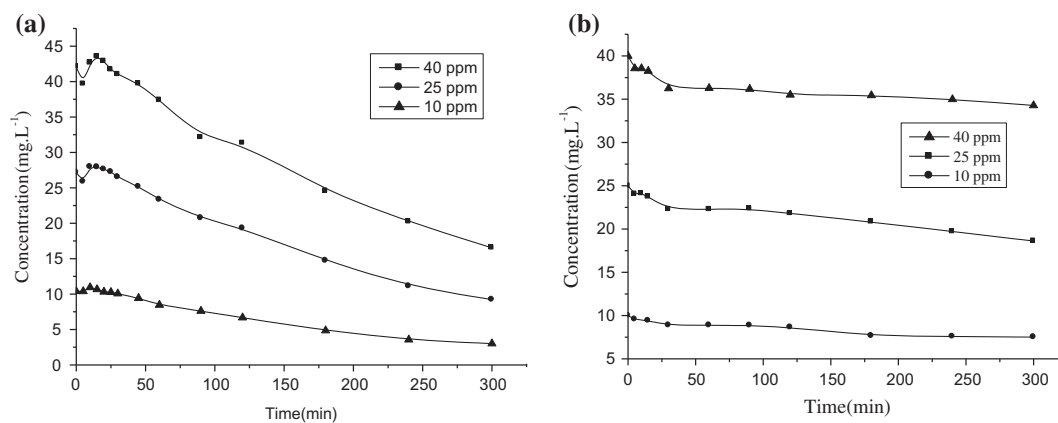


Fig. 3. Decolorization of MG and PCB by direct UV photolysis. Experimental conditions: $\lambda_{irr} = 254$ nm, various concentrations of the two Dyes and for pH equal to 5.8 and 4.5 respectively: (a) MG and (b) BCP. Reaction time: 300 min

the photolytic reaction of MG occurs with a relative high quantum yield [27]. In another hand, the decolorization process decreases as the initial concentration increases for both substrates. Indeed, the results obtained for MG are: 70.77% (10 mg/L), 66.23% (25 mg/L), and 60.36% (40 mg/L); for BCP: 25.8% (10 mg/L), 25.6% (25 mg/L), and 16.6% (40 mg/L). This behavior may be explained by the less participation of photons emitted by the source as the solution becomes more colored or more concentrated.

The decolorization rate of MG using direct photolysis is well represented by the pseudo-zero-order kinetic model in the range of time: 45–300 min.

$$\frac{-d[MG]}{dt} = k_{app} \quad (3)$$

A simple integration lead to relation:

$$[MG]_0 - [MG]_t = k_{app} \cdot t$$

where $[MG]_0$ is the initial concentration (25 mg/L); $[MG]_t$ is the concentration at instant t ; k_{app} is the apparent rate constant.

The fit of this model is reported in Fig. 4.

The value of the correlation coefficient R^2 which is always greater than 0.98 for the pseudo-zero-order demonstrates that the proposed model is in good agreement with the experimental results, and is better than the pseudo-first-order model (data not shown). All parameters like decolorization rate, apparent rate constants (order 0 and 1), and values of R^2 are reported in Table 1.

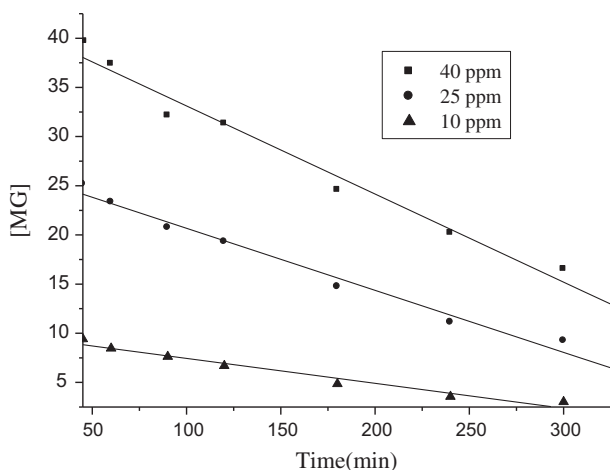


Fig. 4. Kinetics study of MG decolorization by direct UV photolysis process using linear transform C_t vs. time. Experimental conditions: various initial concentrations of the dye, pH 5.8, $\lambda_{irr} = 254$ nm and a reaction time equal to 300 min.

3.1.3. Degradation of MG and BCP by Acetone/UV and H_2O_2 /UV processes

3.1.3.1. Sensitivity of MG and BCP in presence of H_2O_2 and in absence of light. Prior to the study of dyes photo-oxidation by H_2O_2 /UV, it is necessary to know if any reaction may occur when we mix each substrate (constant concentration) with H_2O_2 at various concentrations (from 10^{-1} to 5×10^{-4} M). The evolution of the UV-vis spectra of solutions that contain MG- H_2O_2 and BCP- H_2O_2 mixtures, at constant dyes concentration (25 mg/L), is followed at different concentrations of H_2O_2 and for a reaction time of 240 min. The results depicted in Fig. 5 reveal that BCP is insensitive toward H_2O_2 for the range of the used concentrations whereas MG is sensitive in the presence of this reagent, mainly, for H_2O_2 dose greater than 5×10^{-4} M. Indeed, beyond this value, the classical oxidation route becomes important involving a complete oxidation of MG for $[H_2O_2] = 10^{-1}$ M. However, this part of oxidation is feeble for H_2O_2 concentrations

equal to 5×10^{-4} M and to 10^{-4} M: 19.8 and 15.6%, respectively. Accordingly, these two values will be selected to study the decolorization process of both substrates separately and in the mixture. This choice will allow to situate the proper efficiency of the H_2O_2 /UV system in the bleaching process.

3.1.3.2. Sensitivity of MG and BCP in presence of Acetone in absence of light. Same experiments are performed in the presence of acetone to study the sensitivity of each substrate in the presence of this reagent. Thus, the evolution of the UV-vis spectra of solutions that contain MG-acetone and BCP-acetone mixtures, at constant dyes concentration (25 mg/L), is followed for the highest concentration of acetone (10^{-1} M) and for a reaction time equal to 180 min. As a result, no sensitivity is observed either in MG or in BCP (Fig. 6(a) and (b)).

3.1.4. Photo-oxidation of Methyl green and Bromocresol purple

3.1.4.1. Acetone/UV process. As related by the literature, it appears that photosensitivity is a process which can be considered as a promising route for dye elimination. This technique is used since the obtained efficiency by direct UV photolysis is weak for BCP and not sufficient for MG [28]. To enhance decolorization of both dyes, UV radiations and acetone at different concentrations are combined. Once acetone is excited by UV radiation (254 nm), it leads to an unstable state (or triplet state: Acetone*) with a high energy level (79–82 kcal/mole). As a result, an energy transfer occurs from this excited state of acetone to the dye and via a collision processes. This process is then responsible for the decolorization of the target substrate [28]:



Table 1

Apparent rate constants, correlation coefficient R^2 and rate of decolorization obtained in the UV photolysis process at 254 nm for MG

Methyl green (mg/L)	Rate (%)	R^2 pseudo-zero-order model	Apparent rate constants ($\text{mol L}^{-1} \text{min}^{-1}$)	R^2 pseudo-first-order model	Apparent rate constants (min^{-1})
40	60.36	0.98571	9.37×10^{-2}	0.95517	2.49×10^{-2}
25	66.23	0.99077	6.72×10^{-2}	0.94755	3.45×10^{-2}
10	70.77	0.98491	2.85×10^{-2}	0.95714	4×10^{-2}

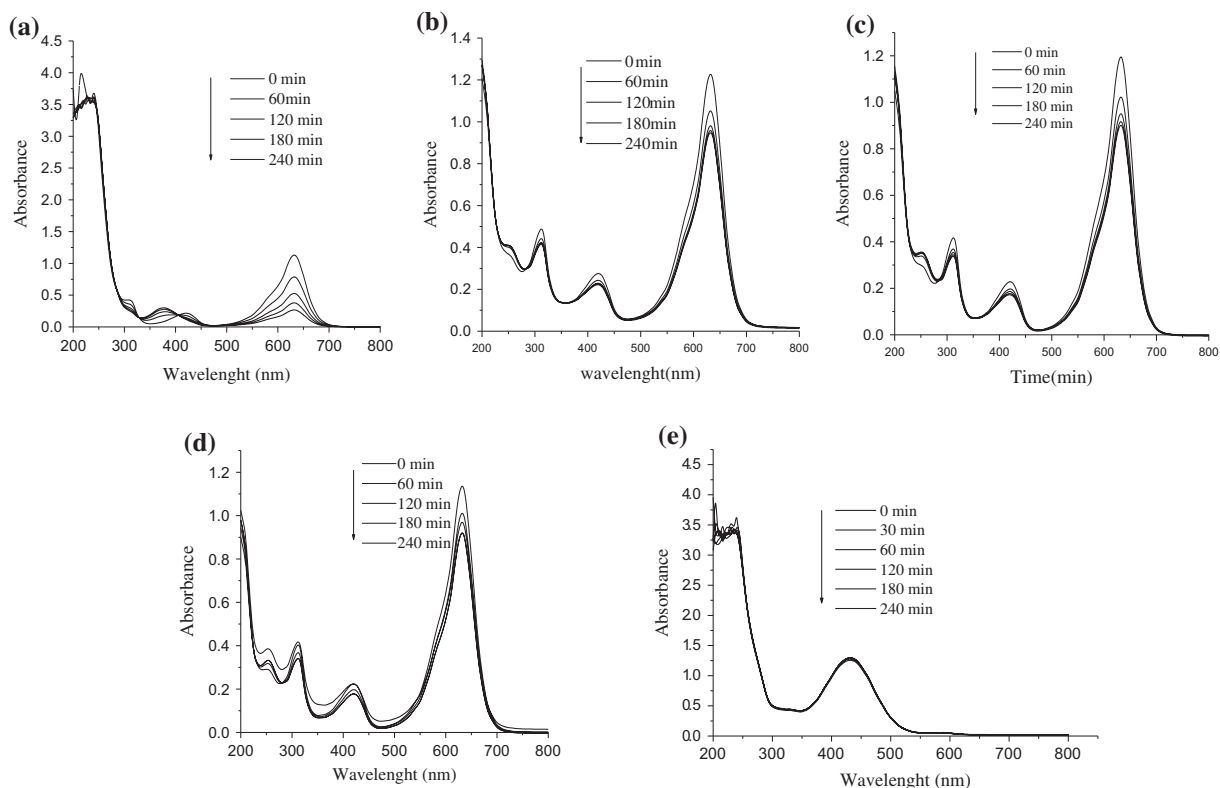


Fig. 5. Sensitivity of MG (25 mg/L) and BCP (25 mg/L), in the presence of different H_2O_2 concentrations, in the absence of light, for pH equal to 5.8 and 4.5, respectively, and for a reaction time equal to 240 min: (a) MG/ H_2O_2 (10^{-1} M), (b) MG/ H_2O_2 (10^{-2} M), (c) MG/ H_2O_2 (5×10^{-4} M), (d) MG/ H_2O_2 (10^{-4} M), and (e) BCP/ H_2O_2 (10^{-1} M).

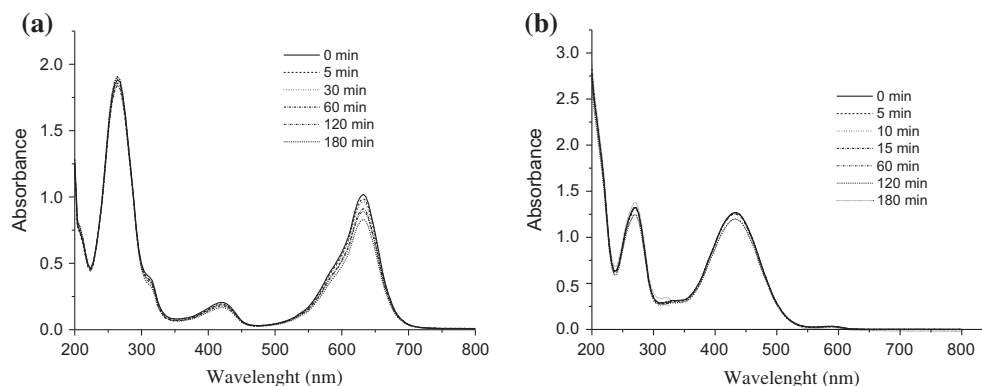


Fig. 6. Sensitivity of MG (25 mg/L) and BCP (25 mg/L) in the presence of acetone (0.1 M), for pH equal to 5.8 and 4.5, respectively, in the absence of light and for a reaction time equal to 180 min: (a) MG/Acetone and (b) BCP/Acetone.

Dye* \rightarrow Decolourization (6)

Various concentrations of acetone ranged from 10^{-1} to 10^{-4} M are used to decolorize aqueous solutions of MG and BCP. The results depicted in Fig. 7(a) and (b) show that acetone is able to decolorize both solutions

of MG and BCP, as the acetone concentration increases. Consequently, MG and BCP are decolorized completely for the highest concentration of this reagent in 60 and 120 min, respectively.

At the end of the energy transfer, we observe that acetone is regenerated as indicated in Eq. (2) and

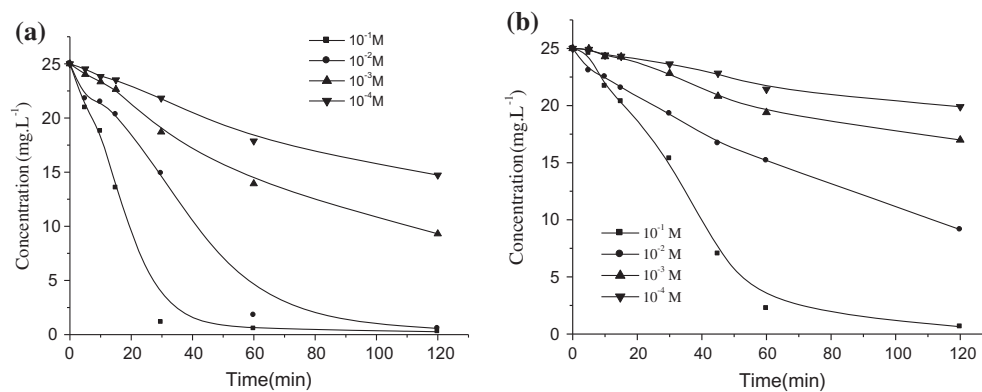


Fig. 7. Decolorization process of MG (25 mg/L) and BCP (25 mg/L) by Acetone/UV process. Experimental conditions: various initial concentrations of Acetone, pH 5.8 and pH 4.5, respectively, reaction time: 120 min and $\lambda_{irr} = 254$ nm. (a) MG and (b) BCP.

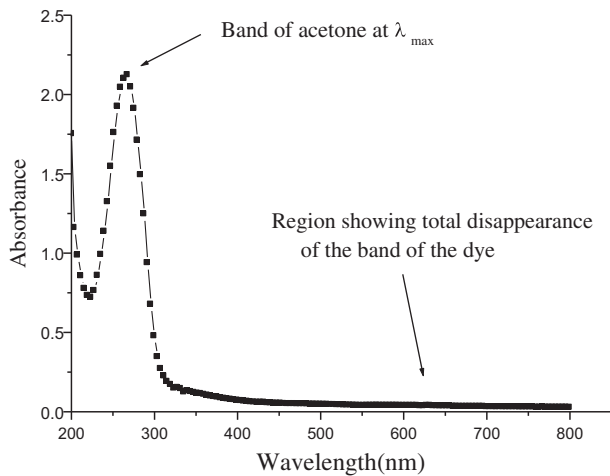


Fig. 8. Spectrum of Acetone obtained at the end of the decolorization of MG by Acetone/UV. The irradiation time is equal to: 120 min and the initial concentration of Acetone equal to: 10^{-1} M.

reported in Fig. 8 which makes the recovery of acetone possible [28].

Furthermore, the disappearance of the dye can be described by a pseudo-first-order kinetics model, mainly, for the concentrations equal to 10^{-1} and 10^{-2} M for both dyes. The choice of these curves is justified because they present a decreased pseudo exponential shape (Fig. 9(b)):

$$-\frac{dC}{dt} = k_{app} \cdot C \quad (7)$$

The integration of this expression yields the following result:

$$\ln\left(\frac{C_0}{C}\right) = k \cdot t \quad (8)$$

As a result, k_{app} values (apparent rate constants) are deduced from the slopes of the plot: $\ln(C_0/C)$ vs. time. In these conditions, the value of R^2 which is above 0.98 shows that the color removal of MG and BCP using acetone/UV process follows well the pseudo-first-order kinetic model, mainly, for concentrations in acetone equal to 10^{-2} and 10^{-1} M (Fig. 9(a) and (b)). The values of R^2 , the bleaching rate (%), and the apparent rate constant (min^{-1}) are summarized in Table 2.

The obtained results in this research are similar to those reported in the literature [29].

3.1.4.2. UV/H₂O₂ process. Better results are obtained when H₂O₂ is combined with UV radiation at 254 nm. This combination facilitates the photodecomposition of H₂O₂ into radicals $\cdot\text{OH}$ which are powerful oxidants since they have high potential oxidation (≈ 2.8 volt). [30]. As expected, BCP (pH 4.5) and MG (pH 5.8) are completely decolorized for $[\text{H}_2\text{O}_2] = 10^{-2}$ M and $[\text{H}_2\text{O}_2] = 5 \times 10^{-4}$ M for a reaction time of 30 and 80 min, respectively, whereas the rate of decolorization of MG reaches 92% for $[\text{H}_2\text{O}_2] = 10^{-4}$ M after 2-h reaction time (Fig. 10(a) and (b)). As a result, the bleaching time is much longer than that obtained with BCP, revealing a feeble participation of radicals $\cdot\text{OH}$. For PCB, this process becomes more rapid as the concentration of H₂O₂ increases gradually, due to an important production of radicals $\cdot\text{OH}$ in the medium. However, for the highest value in H₂O₂ concentration (10^{-1} M), a decrease in the depletion rate is observed.

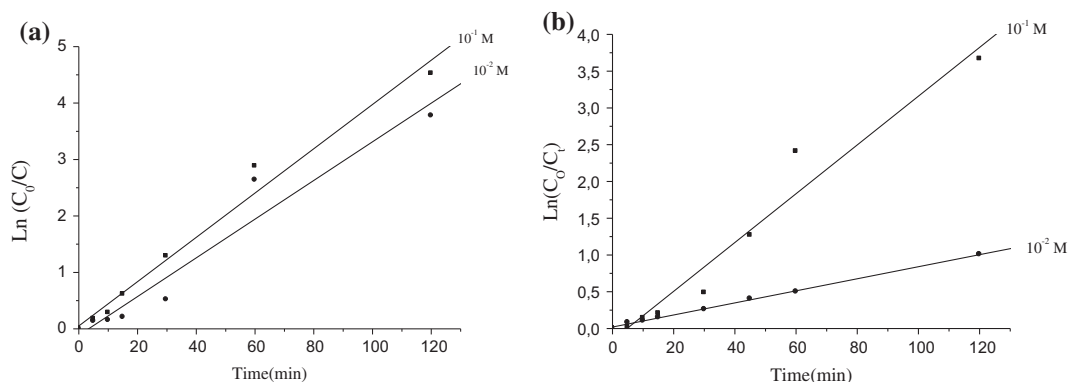


Fig. 9. Kinetics study of the decolorization process of both dyes (25 mg/L) by Acetone/UV at 254 nm, using linear transform: $\ln C_0/C$ vs. time and two different initial concentrations of acetone: 10^{-1} M and 10^{-2} M. The pH is equal to 5.8 for MG and 4.5 for BCP, respectively. The reaction time is equal to 120 min: (a) MG and (b) BCP.

Table 2

Values of apparent rate constants, correlation coefficient R^2 and rate of decolorization obtained with Acetone/UV process at 254 nm for MG and BCP respectively

Dye (mg/L)	Acetone (Mol/l)	Rate (%)	R^2	Apparent rate constants (min^{-1})
MG (25 mg/L)	10^{-1}	100	0.97236	3.42×10^{-2}
	10^{-2}	98.2	0.99529	4.07×10^{-2}
BCP (25 mg/L)	10^{-1}	97.44	0.9791	3.3×10^{-2}
	10^{-2}	63.48	0.99916	8.2×10^{-3}

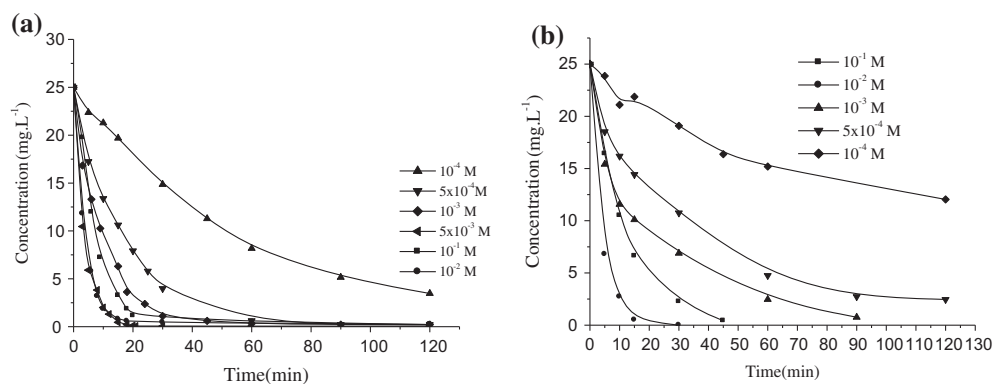
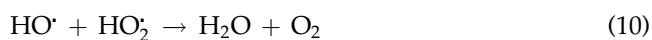
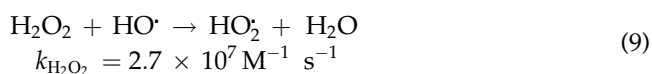


Fig. 10. Decolorization process of MG (25 mg/L) and BCP (25 mg/L) by $\text{H}_2\text{O}_2/\text{UV}$ process. Experimental conditions: various initial concentrations of H_2O_2 , pH 5.8 and 4.5, respectively, reaction time: 120 min and $\lambda_{\text{irr}} = 254$ nm. (a) MG and (b) BCP.

This behavior may be due to scavenging effect of radicals $\cdot\text{OH}$ by an excess of H_2O_2 [31,32]:



We observe that when $\text{H}_2\text{O}_2/\text{UV}$ is used in optimum conditions, it become efficient in the decolorization process for both dyes although they have different structures. Similar results are related in the literature [25,33–36].

A pseudo-first-order kinetic model is used to describe the decolorization process [37]:

$$-\frac{dC_{AY}}{dt} = k_1 C_{DY} C_{HO\cdot} \quad (11)$$

where C_{dye} and $C_{HO\cdot}$ represent substrate, hydroxyl radical concentrations. Furthermore, we consider that hydroxyl radical is constant because it reaches equilibrium state rapidly (process of steady state). Therefore, the expression rate of the above Eq. (13) may be reduced to a simple kinetic model.

In this case, the disappearance of the dye can be described by a pseudo-first-order kinetics Fig. 9(b):

$$-\frac{dC}{dt} = k_{app} \cdot C \quad (12)$$

The integration of this expression yields the following result:

$$\ln\left(\frac{C_0}{C}\right) = k \cdot t \quad (13)$$

where C_0 is the initial concentration of the substrate, C is concentration at instant t , and k_{app} is the pseudo-first-order kinetic constant. The apparent rate constants are deduced from the plot of $\ln(C_0/C)$ vs. time. The straight lines obtained in the case of PCB, mainly, for the set of the used H_2O_2 concentrations, confirm the reasonable choice of the pseudo-first-order kinetic model. In another hand, the value of the apparent rate constant increases as the concentration of H_2O_2 increases (Table 3 and Fig. 11(b)) revealing a high participation of radicals $\cdot OH$ in the bleaching process.

The same method is also applied for the kinetics study of the MG decolorization (25 mg/L) using only two types of concentrations: 5×10^{-4} and 10^{-4} M (Fig. 11(a)). All experimental results are displayed in this table.

3.1.5. Spectral evolution of MG and BCP by UV/ H_2O_2

The changes in absorption spectra of MG and BCP solutions during the treatment by H_2O_2 /UV process, at different reaction times, are reported in Fig. 12(a)–(c). Before this treatment, the UV–visible spectrum of each dye is constituted by absorption bands positioned in UV and visible regions. It is clearly observed that the absorption peaks located at 632 nm for MG and at 432 nm for BCP, decrease rapidly and nearly disappear in 120, and 20 min under H_2O_2 /UV and with respect to the used concentrations in H_2O_2 : 10^{-4} M, 5×10^{-4} M for MG, and 10^{-2} M for BCP. The bands located in the UV region for both dyes are also observed to decrease gradually but at a lower rate comparatively to the visible bands. This evolution is mainly attributed to the attack of radicals $\cdot OH$ on π – π^* transitions related to the benzene rings causing the destruction of the conjugated π systems, n – π^* transitions of S=O group, and bonds like C–O and S–O. As a result, a total decolorization occurs for both dyes [38]. In this part, all experiments are conducted at pH 4.5 for PCG and at pH 5.8 for MG

3.2. Case of dye mixtures

3.2.1. UV–vis spectrum of the mixture

The UV–visible spectrum of the dyes mixture was recorded in the same spectrophotometer for wavelength ranging from 200 to 800 nm and for an equal concentration of each substrate: 25 mg/L. The two bands are clearly separated (no overlapping) and their maxima are distant from each other (Fig. 13). Besides, no shift in absorption bands was observed but a slight decrease of the absorption maximum in each peak for both compounds revealing thereby a negligible interaction between them. The absorption measurement is carried out at 632 nm and at 432 nm, for pH equal to 4.4.

Table 3

Values of apparent rate constants, correlation coefficient R^2 and rate of decolorization obtained with H_2O_2 /UV process at 254 nm for MG and BCP respectively

Dye (mg/L)	H_2O_2 (Mol/l)	Rate (%)	R^2	Apparent rate constants (min^{-1})
MG (25 mg/L)	5×10^{-4}	99.1	0.97089	4.3×10^{-2}
	10^{-4}	86.2	0.99788	1.68×10^{-2}
BCP (25 mg/L)	10^{-1}	98.44	0.99699	8.85×10^{-2}
	10^{-2}	100	0.99345	2.53×10^{-1}
	10^{-3}	97	0.99336	3.5×10^{-2}
	10^{-4}	51.44	0.97043	6×10^{-3}

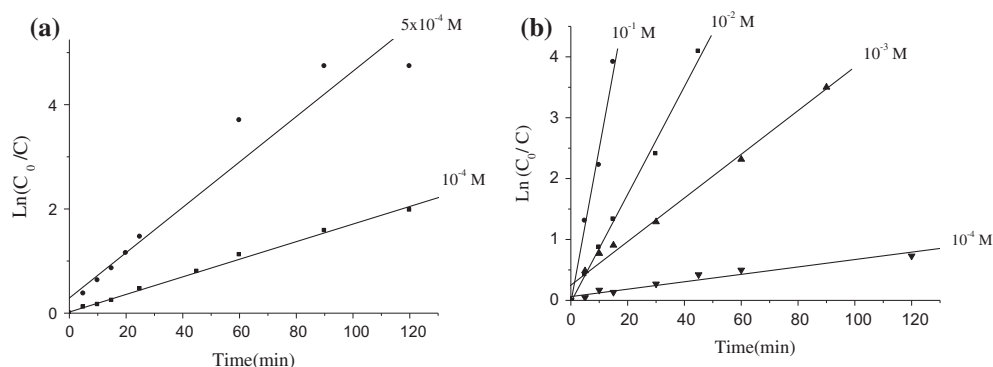


Fig. 11. Kinetics study of the decolorization process of both dyes (25 mg/L) by H_2O_2/UV at 254 nm, using linear transform: $\ln C_0/C$ vs. time and different initial concentrations of H_2O_2 . The pH is equal to 5.8 for MG and 4.5 for BCP, respectively. The reaction time is equal to 120 min: (a) MG and (b) BCP.

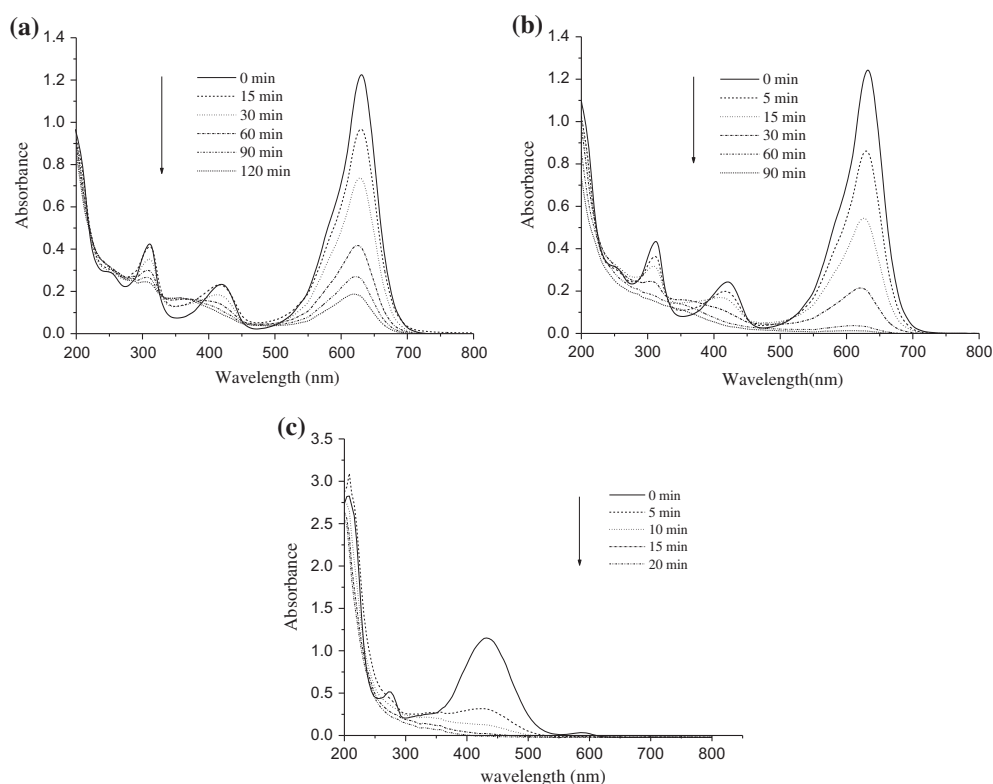


Fig. 12. Spectral Evolution of MG and BCP during UV/H_2O_2 treatment at 254 nm, taken at equal concentrations ($[dye]_0 = 25$ mg/L) and at their initial pH; 5.8 and 4.5, respectively. (a) MG: $[H_2O_2]_0 = 10^{-4} M$, (b) MG: $[H_2O_2]_0 = 5 \times 10^{-4} M$, and (c) BCP: $[H_2O_2]_0 = 10^{-2} M$.

3.2.2. Direct photolysis of the dye mixture

The direct UV photolysis of the dyes mixture at 254 nm is performed in the same reactor with solution containing different concentrations of both substrates. The Fig. 14 shows the evolution of the decolorization of the mixture during its photolysis treatment which

contains MG at constant concentration (25 mg/L) and PCB at various concentrations in the range of 10–30 mg/L. The results indicate that the decolorization rate of MG decreases slightly and reaches 40% for the highest concentration of PCB. However, the inverse case characterized by a constant concentration of BCP (25 mg/L) and various concentrations of MG

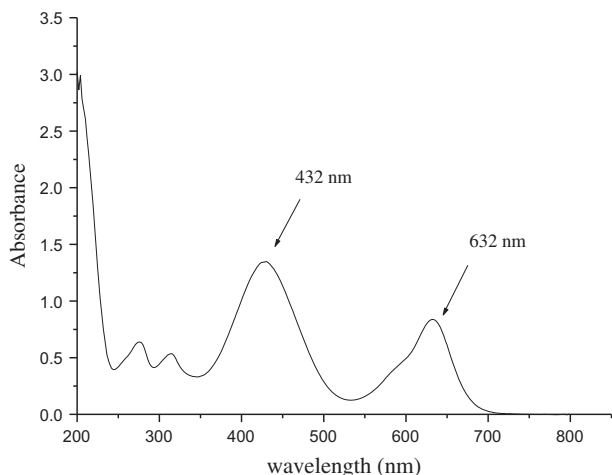


Fig. 13. UV-vis spectrum of the MG and BCP mixture dyes taken in the same concentrations: 25 mg/L and for a pH equal to 4.4.

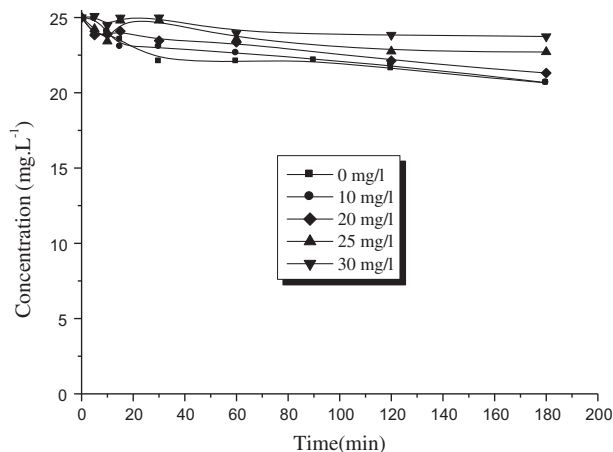


Fig. 15. Effect of the concentration of BCP on the photolytic decolorization of MG at 25 mg/L, and at 254 nm and for a reaction time: 180 min.

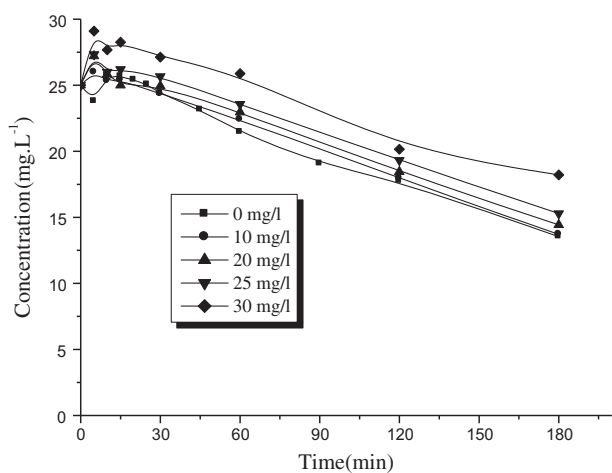


Fig. 14. Effect of the concentration of BCP on the photolytic decolorization of MG at 25 mg/L, and at 254 nm and for a reaction time: 180 min.

taken in the same range show a negligible elimination rate, (Fig. 15). This feature can be attributed mainly for MG, to the diminution of the absorbance as the solution becomes more concentrated or more colored.

3.2.3. Photooxydation of the dye mixture

3.2.3.1. Acetone/UV process. The same mixtures are treated by Acetone/UV process using similar experimental conditions. It can be seen, that decolorization rate of MG (25 mg/L) diminishes as the concentration of BCP augments to reach finally 80% for the highest

concentration of BCP for a reaction time of 120 min (Fig. 16). This decrease is linked to the less participation of photons emitted by the source. As a result, the excitation of the sensitizer becomes feeble and allows an insufficient energy transfer to bleach the solution. In this case, the photons can be disturbed as the solution becomes more and more concentrated. Same behavior is observed in the case of BCP (Fig. 17).

The results established in these experiments demonstrate the usefulness of the process acetone/UV at 254 nm in the decolorization rate of both dye mixtures although they have different structures. Undeniably, they disappear almost completely in the same reaction time (≈ 90 min), principally, for 10 and 20 mg/L for each dye. Additionally, no change in the pseudo-first-order kinetic model is observed in the mixture where all experimental data are reported in Table 4 in terms of R^2 values which are generally greater than 0.97. This table reports also the rate efficiency and the apparent rate constants.

3.2.3.2. UV/H₂O₂ process. The bleaching process of the mixtures is achieved using H₂O₂/UV at 254 nm and under the same experimental conditions. The Fig. 18(a) shows decolorization rate of MG at constant concentration in the presence of BCP at various concentrations in the range of 10–30 mg/L. As a result, the efficiency decreases as the concentration of BCP increases gradually and reaches 40% for the highest PCB dosage: 30 mg/L [39]. The Fig. 19(a) shows also the same evolution for the opposite mixture but with a more pronounced decolorization rate (Table 5). These results can be explained by a feeble production of $\cdot\text{OH}$ since the H₂O₂ dosage is weak (10^{-4} M) and by

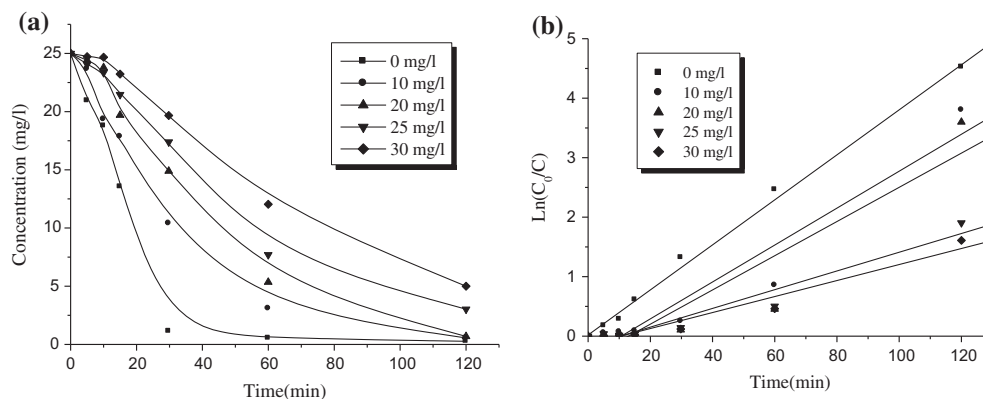


Fig. 16. (a) Effect of the concentration of BCP on decolorization process of MG at 25 mg/L in presence of Acetone/UV process at 254 nm and for [Acetone] = 10^{-1} M and (b) Kinetics study of MG decolorization using linear transform $\ln(C_0/C_t)$ vs. time. Reaction time: 120 min.

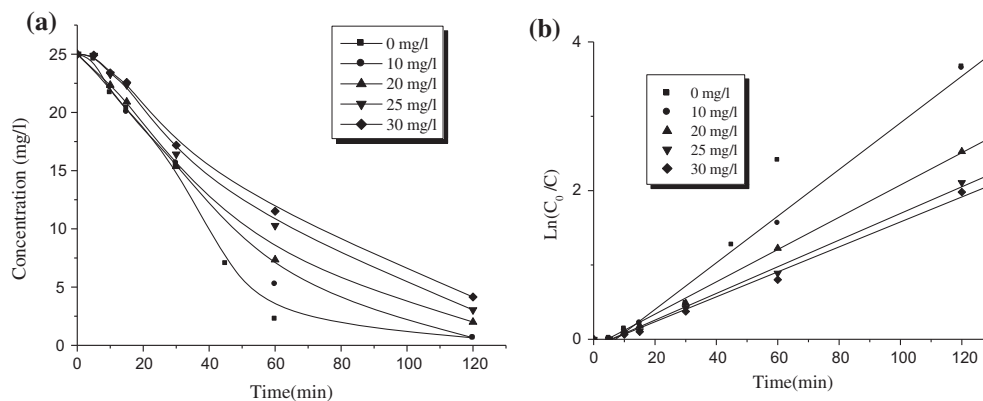


Fig. 17. (a) Effect of the concentration of MG on Decolorization process of the BCP at 25 mg/L in presence of Acetone/UV process at 254 nm and for [Acetone] = 10^{-1} M and (b) Kinetics study of BCP decolorization using linear transform $\ln(C_0/C_t)$ vs. time. Reaction time: 120 min.

Table 4

Values of apparent rate constants, correlation coefficient R^2 and rate of decolorization of both mixtures obtained by Acetone/UV process at 254 nm

MG (mg/L)	BCP (mg/L)	Rate (%)	R^2	Apparent rate constants (min^{-1})
25	0	100	0.97236	3.42×10^{-2}
	10	97.77	0.95962	3.10×10^{-2}
	20	97.26	0.92919	2.87×10^{-2}
	25	85.1	0.96857	1.57×10^{-2}
	30	80	0.97384	1.34×10^{-2}
0	25	97.44	0.9791	3.3×10^{-2}
10		97.39	0.99322	3.13×10^{-2}
20		92	0.99819	2.17×10^{-2}
25		87.83	0.99655	1.79×10^{-2}
30		86.19	0.99535	1.67×10^{-2}

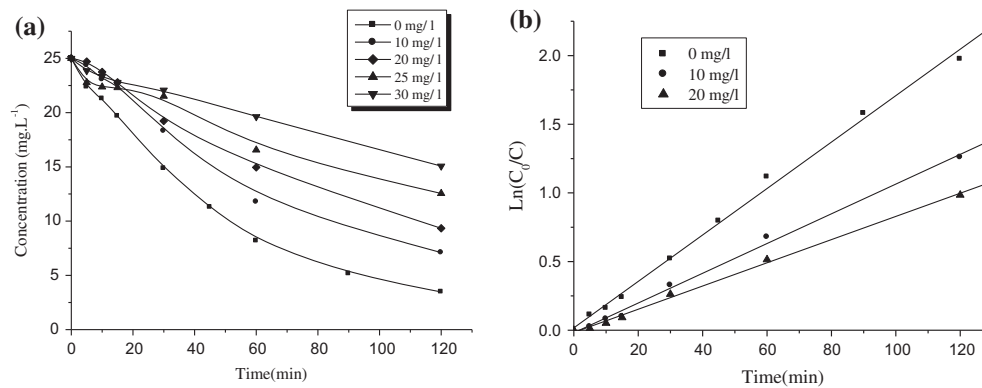


Fig. 18. (a) Effect of the concentration of BCP on decolorization process of MG at 25 mg/L in presence of H_2O_2 /UV process at 254 nm and for $[H_2O_2] = 10^{-4}$ M. (b) Kinetics study of MG decolorization using linear transform $\ln(C_0/C_t)$ vs. time. Reaction time: 120 min.

Table 5

Values of apparent rate constants, correlation coefficient R^2 and rate of decolorization of both mixtures obtained by UV/H_2O_2 (10^{-4} M) process at 254 nm

MG (mg/L)	BCP (mg/L)	Rate (%)	R^2 Pseudo-first-order	Apparent rate constants (min^{-1})
25	0	86.2	0.99792	1.69×10^{-2}
	10	71.6	0.99781	1.08×10^{-2}
	20	62.68	0.98948	5.5×10^{-3}
	25	49.56	0.99656	4×10^{-3}
	30	40	0.99847	8.4×10^{-3}
0	25	51.44	—	—
10		44	—	—
20		38.2	—	—
25		34.96	—	—
30		32.08	—	—

the behavior of photons which become more disturbed when the concentration of the solution is high. In these conditions, the solution is not permeable to UV radiations [34]. Consequently, the oxidation of dye mixture slows down.

Once again, no change in the pseudo-first-order kinetic model is observed when the mixture is treated by H_2O_2 /UV and where the fitting of the experimental data is reported in Table 5 in terms of R^2 values which are always greater than 0.97. This behavior is not observed in the inverse case since the curves do not present a real decreased exponential shape and consequently, they cannot describe this model (Figs. 18(b) and 19(b)). This table summarizes also the rate efficiency (%) and the apparent rate constants.

As mentioned before, the bibliographic data linked to the treatment of the dye mixtures by photochemical methods are limited, mainly, in homogeneous medium. Nevertheless, they are available in heterogeneous medium [15,40,41].

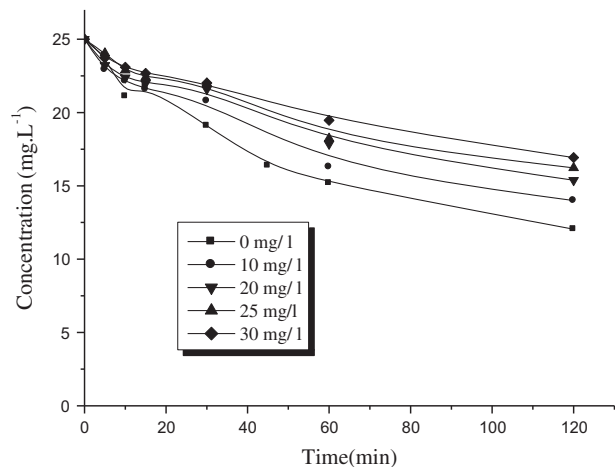


Fig. 19. Effect of the concentration of MG on decolorization process of the BCP at 25 mg/L in presence of H_2O_2 /UV process at 254 nm and for $[H_2O_2] = 10^{-4}$ M. Reaction time: 120 min.

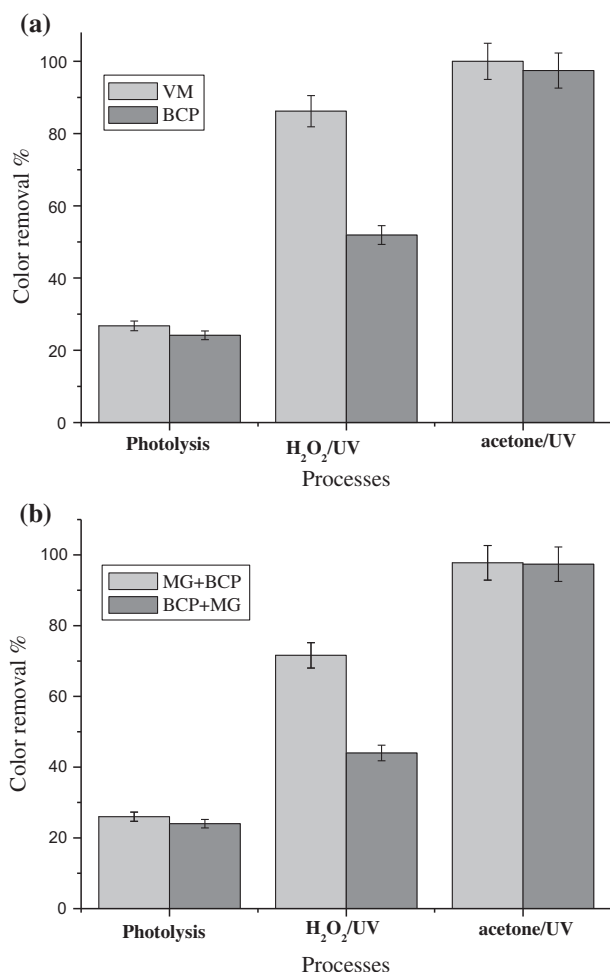


Fig. 20. Comparison of the decolorization process of the two dyes MG and BCP using $[H_2O_2] = 10^{-4}$ M and $[Acetone] = 10^{-1}$ M. Reaction time: 120 min. (a) In mono system: $[MG] = [BCP] = 25$ mg/L, (b) In binary system: $[MG] = (25$ mg/L + $[BCP] = 10$ mg/L) and $[BCP] = (25$ mg/L + $[MG] = 10$ mg/L).

4. Comparison of the effectiveness of the different systems used

The histograms presented in Fig. 20(a) and (b), show the efficiency of the decolorization process of the two dyes treated by the three photochemical techniques used in single and binary systems. The comparison of the decolorization process obtained from photolysis, H₂O₂/UV, and Acetone/UV and after 120 min reveals that the efficiency decreases in the following order: Acetone/UV > H₂O₂/UV > photolysis. In these conditions, the dominant process among them and in both cases is Acetone/UV.

5. Conclusion

The aim of this work is to test some photochemical processes to decolorize two dyes, taken in mono and binary systems in aqueous homogeneous medium. First, both substrates are treated separately by direct UV photolysis at 254 nm. The experimental results indicate that MG (25 ppm) undergoes to an acceptable decolorization rate (66%) but after a relatively long reaction time (300 min), whereas for BCP (25 ppm) this process is weak (around 25%) for the same reaction time. A real improvement is observed when both substrates are treated either by acetone/UV (photosensitization) or by H₂O₂/UV (an advanced oxidation process). In these conditions, a total decolorization is obtained as well as for BCP as for MG, for $[Acetone] = 10^{-1}$ M. Similar result is also obtained only with MG for $[H_2O_2] = 5 \times 10^{-4}$ M. However, a good knowledge of the sensitivity of each dyes towards H₂O₂ and acetone in dark conditions is required. It allows to situate the intrinsic value of both processes in order to minimize the contribution the chemical oxidation route. This is the case of MG where the decolorization rate reaches 85% for $[H_2O_2] = 10^{-4}$ M after 2-h reaction time and 100% for $[H_2O_2] = 10^{-1}$ M in 20 min. In another hand, the treatment of the mixture becomes rather complicated comparatively to the separated dyes. According to the experimental results, we observe that the decolorization process decreases as the concentration of the solution becomes high. In these conditions, this solution is not permeable to UV radiations. Thus, among these processes, acetone/UV seems to be the best system in comparison to the direct UV photolysis and H₂O₂/UV. Additionally, the decolorization process due to direct UV photolysis, Acetone/UV, and H₂O₂/UV is correctly described by pseudo-zero-order and by pseudo-first-order models for each dye taken separately. In the mixture, the latter model remains almost unchanged.

References

- [1] S.K. Khare, R.M. Srivastava, K.K. Panday, V.N. Singh, Removal of basic dye (crystal violet) from water using wollastonite as adsorbent, *Environ. Technol. Lett.* 9 (1988) 1163–1172.
- [2] M.N. Ahmed, R.N. Ram, Removal of basic dye from waste-water using silica as adsorbent, *Environ. Pollut.* 77 (1992) 79–86.
- [3] F. Perineau, J. Molinier, A. Gaset, Adsorption de colorants ioniques sur le dechet lainier de carbonisage (Adsorption of ionic dyes on wool carbonizing waste), *Water Res.* 17 (1983) 559–567.
- [4] J. Paprowicz, S. Słodczyk, Application of biologically activated sorptive columns for textile waste water treatment, *Environ. Technol. Lett.* 9 (1988) 271–280.

- [5] R.R. Bowers, W.W. Eckenfelder, J. Gaddipati, R.M. Morsen, Toxicity reduction in industrial wastewater discharges, *Pollut. Eng.* 2 (1988) 68–72.
- [6] Y. Yang, C. Ladisch, M.R. Ladisch, Cellulosic adsorbents for treating textile mill effluents, *Enzyme Microb. Technol.* 10 (1988) 632–636.
- [7] O. Dusart, D. Marmier-Dussoubs, B. Serpaud, Removal of industrial dyes on peat, sawdust, graft cellulose and charcoal, *La tribune de l'eau* 44 (1991) 15–22.
- [8] A. Savino, G. Angeli, Photodynamic inactivation of *E. coli* by immobilized or coated dyes on insoluble supports, *Water Res.* 19 (1983) 1465–1469.
- [9] I.K. Chandra, Y.-H. Ju, A. Ayucitra, S. Ismadji, Evans blue removal from wastewater by rarasaponin-bentonite, *Int. J. Environ. Sci. Technol.* 10 (2013) 359–370.
- [10] G. McKay, B. Al-Duri, Activated carbon for removal of basic dyes from effluents, *Colourage* 35 (1988) 24–28.
- [11] F.Z. Meghlaoui, M. Bouhelassa, N. Hadj-Salah, S. Bekkouche, Study of adsorption of phenol on titanium oxide (TiO₂), *Desalination* 166 (2004) 355–362.
- [12] C.H. Wu, Adsorption of reactive dye onto carbon nanotubes: Equilibrium, kinetics and thermodynamics, *J. Hazard. Mater.* 144 (2007) 93–100.
- [13] K.C. Chen, J.Y. Wu, C.C. Huang, Y.M. Liang, S.C.J. Hwang, Decolorization of azo dye using PVA-immobilized microorganisms, *J. Biotechnol.* 101 (2003) 241–252.
- [14] Y.B. Phatake, R.J. Marathe, M.S. Shejul, Use of fungi isolated from textile effluent for degradation of synthetic dyes and optimization of degradation process, *Glob. J. Bio-sci. Biotechnol.* 4 (2015) 314–319.
- [15] A.K. Gupta, A. Pal, C. Sahoo, Photocatalytic degradation of a mixture of Crystal Violet (Basic Violet 3) and Methyl Red dye in aqueous suspensions using Ag⁺ doped TiO₂, *Dyes Pigm.* 69 (2006) 224–232.
- [16] G.V. Buxton, C.L. Greenstock, W.P. Helman, A.B. Ross, Critical review of literature for rate constants for reaction of chemical oxidants with inorganic and organic pollutants, *J. Phys. Chem.* 17 (1988) 513–886.
- [17] S.H. Gau, F.S. Chang, Improved Fenton method to remove recalcitrant organics in landfill leachate, *Water Sci. Technol.* 34 (1996) 455–462.
- [18] M.S. Lucas, J.A. Peres, Decolorization of the azo dye Reactive Black 5 by Fenton and photo-Fenton oxidation, *Dyes Pigm.* 71 (2006) 236–244.
- [19] S. Fassi, K. Djebbar, I. Bousnoubra, H. Chenini, T. Sehili, Oxidation of bromocresol green by different advanced oxidation processes: Fenton, Fenton-like, photo-Fenton, photo-Fenton-like and solar light. Comparative study, *Desalin. Water Treat.* 52 (2014) 4982–4989.
- [20] A. Aleboyh, H. Aleboyeh, Effect of gap size and UV dosage on decolorization of C.I. acid orange 7 by UV/H₂O₂ process, *J. Hazard. Mater.* 133 (2006) 167–171.
- [21] J.C. Milano, P. Lose-Berdot, J.L. Vernet, Photo-oxidation du vert de Malachite en milieu aqueux en présence de peroxyde d'hydrogène (Photo-oxidation of malachite green in aqueous medium in the presence of hydrogen peroxide: Kinetic and mechanism), *J. Environ. Technol.* 16 (1995) 329–341.
- [22] S. Al-Qaradawi, R.S. Salman, Photocatalytic degradation of methyl orange as a model compound, *J. Photochem. Photobiol. A: Chem.* 148 (2002) 161–168.
- [23] T. Sauer, G. Gesconeto Neto, H.J. José, R.F.P.M. Moreira, Kinetic of photocatalytic degradation of reactive dyes in a TiO₂ slurry reactor, *J. Photochem. Photobiol. A: Chem.* 149 (2002) 147–154.
- [24] R. Djellabi, M.F. Ghorab, Solar photocatalytic decolorization of crystal violet using supported TiO₂: Effect of some parameters and comparative efficiency, *Desalin. Water Treat.* 53 (2013) 1–7.
- [25] K. Djebbar, S. Aliouche, H. Chenini, T. Sehili, Decolorization of an azoïque dye (congo red) by photochemical methods in homogeneous medium, *Desalination* 250 (2009) 76–86.
- [26] N. Barka, L'élimination des colorants de synthèse par adsorption sur un phosphate naturel et par dégradation photocatalytique sur TiO₂ supporté (Elimination of synthetic dyes by adsorption on natural phosphate and by photocatalytic degradation on supported TiO₂), PhD thesis, N° 65/2008, Faculty of Science, University Ibn Zohr Agadir, Morocco, 2008, pp. 83–85.
- [27] K. Djebbar, T. Sehili, P. Mazellier, J. De Laat, Phototransformation of diuron in aqueous solution by UV irradiation in the absence and in the presence of H₂O₂, *Environ. Technol.* 24 (2003) 479–489.
- [28] W. Chu, S.M. Tsui, Photo-sensitization of diazo disperse dye in aqueous acetone, *Chemosphere* 39 (1999) 1667–1677.
- [29] F. Banat, S. Al-Asheh, M. Al-Rawashdeh, M. Nusair, Photodegradation of Methylene blue dye by the H₂O₂/UV and acetone/UV oxidation processes, *Desalination* 181 (2005) 225–232.
- [30] O. Legrini, E. Oliveros, A.M. Braun, Photochemical processes for water treatment, *Chem. Rev.* 93 (1993) 671–698.
- [31] M.A. Behnajady, N. Modirshahla, M. Shokri, Photodestruction of Acid Orange 7 (AO7) in aqueous solutions by UV/H₂O₂: Influence of operational parameters, *Chemosphere* 55 (2004) 129–134.
- [32] C. Galindo, P. Jacques, A. Kalt, Photodegradation of the amino azo benzene acid orange 52 by three advanced oxidation processes: UV/H₂O₂, UV/TiO₂ and VIS/TiO₂: Comparative mechanistic and kinetic investigations, *J. Photochem. Photobiol. A: Chem.* 141 (2001) 47–56.
- [33] S. Aliouche, K. Djebbar, T. Sehili, Removal of an azo dye (Alizarin yellow) in homogeneous medium using direct photolysis, Acetone/UV, H₂O₂/UV, S₂O₈²⁻/UV, H₂O₂/S₂O₈²⁻/UV and S₂O₈²⁻/heat, *Desalin. Water Treat.* (in press) doi: 10.1080/19443994.2015.1090915.
- [34] E. Basturk, M. Karatas, Decolorization of anthraquinone dye Reactive Blue 181 solution by UV/H₂O₂ process, *J. Photochem. Photobiol. A: Chem.* 299 (2015) 67–72.
- [35] A. Aleboyeh, M.E. Olya, H. Aleboyeh, Electrical energy determination for an azo dye decolorization and mineralization by UV/H₂O₂ advanced oxidation process, *Chem. Eng. J.* 137 (2008) 518–524.
- [36] C. Tan, N. Gao, Y. Deng, Y. Zhang, Degradation of antipyrine by UV, UV/H₂O₂ and UV/PS, *Chem. Eng. J.* 216 (2013) 1008–1016.
- [37] H.-Y. Shu M.-C. Chang, H.-J. Fan, Decolorization of azo dye acid black 1 by the UV/H₂O₂ process and optimization of operating parameters, *J. Hazard. Mater. B* 113 (2004) 201–208.
- [38] J.-H. Sun, S.-P. Sun, G.-L. Wang, L.-P. Qiao, Degradation of azo dye Amido black 10B in aqueous solution by Fenton oxidation process, *Dyes Pigm.* 74 (2007) 647–652.

- [39] N. Barka, A. Assabbane, A. Nounah, A. Albourine, Y. Ait-Ichou, Dégradation photo catalytique de deux colorants séparés et en mélange binaire par TiO₂-supporte (Photocatalytic degradation of two dyes separated and in binary mixture by supported TiO₂), *Rev. Sci. Technol A, B* 27 (2008) 9–16.
- [40] K. Sahel, N. Perol, F. Dappozze, M. Bouhent, Z. Derriche, C. Guillard, Photocatalytic degradation of a mixture of two anionic dyes: Procion Red MX-5B and Remazol Black 5 (RB5), *J. Photochem. Photobiol. A: Chem.* 212 (2010) 107–112.
- [41] B. Hemmateenejad, P. Shadabipour, T. Khosousi, M. Shamsipur, Chemometrics investigation of the light-free degradation of methyl green and malachite green by starch-coated CdSe quantum dots, *J. Ind. Eng. Chem.* 27 (2015) 384–390.